Experimental investigation of harmonic and subharmonics synchronization of 40 GHz mode-locked quantum-dash laser diodes

Ramón Maldonado-Basilio, Sylwester Latkowski, Severine Philippe, and Pascal Landais*

School of Electronic Engineering, Dublin City University, Glasnevin, Dublin 9, Ireland

*Corresponding author: landaisp@eeng.dcu.ie

Synchronization of a 40 GHz quantum-dash mode-locked (ML) Fabry–Perot laser diode with optically injected pulse streams is experimentally studied. Injected signals consist of nonmodulated and modulated trains of 1:6 ps pulses at various repetition rates, ranging from 10 to 160 GHz and 10 to 160 Gbps, respectively. Subharmonic, fundamental, and harmonic synchronization of the ML laser allows retrieval of stable 40 GHz clock pulses featuring a width of 1:8 ps. Frequency components at 10 and 20 GHz do not create any amplitude modulation on the recovered 40 GHz clock pulses when injecting signals at 10 and 20 GHz=Gbps. In addition, external synchronization of the laser with pulse streams at 80 and 160 GHz=Gbps is sustained despite the absence of significant components at or below 40 GHz.

Optical injection in passively mode-locked (ML) semi-conductor lasers has been extensively studied for a variety of applications, synchronization (or so-called all-optical clock recovery) being among the most attractive uses for optical time division multiplexed networks. Synchronization of passively ML lasers to injected data streams at the line rate is indispensable for reamplification, retiming, and reshaping functions, while subharmonic operation is essential for demultiplexing. A number of ML laser structures (either single or multisection de-vices), experimental setups, and data rates have been investigated for synchronization [1–3]. In recent studies, quantum-dash (QDash) and quantum-dots (QD) Fabry– Perot (FP) semiconductor lasers have been shown to be good candidates for implementing such functions due to their low power consumption, compact size, fast carrier dynamics, as well as broad and nearly flat gain spectrum around 1550 nm [4]. In comparison to their bulk and quantum-well counterparts, the very narrow beat-tone linewidth exhibited by QDash/QD devices in passive mode-locking operation leads to a smaller timing jitter in short pulse generation or a reduction of timing jitter with respect to that of the injected pulse data stream in all-optical clock-recovery applications [5,6]. The performance of the recovered clock has usually been assessed either by remodulating it with the original data stream and implementing bit-error-rate measurements [7] or analyzing the linewidth of the beat tones and retrieving the root mean square timing jitter [8]. The aim of this work is to investigate the synchronization performance of a QDash ML laser subject to optical injection of nonmodulated and modulated trains of 1:6 ps pulses at various repetition rates, ranging from 10 to 160 GHz and 10 to 160 Gbps, respectively. Frequency and time-domain traces of the recovered clock pulses are analyzed in terms of the spectral components of the injected signals. Following our experiment, it is found that the subharmonic (injection at 10 and 20 GHz/Gbps), fundamental (injection at 40 GHz/Gbps), and harmonic (injection at 80 and 160 GHz=Gbps) synchronization of the QDash ML la-ser allow retrieval of stable 40 GHz clock pulses featuring a width of 1:8 ps as well as a nearly linear flat phase measured throughout the FWHM of the pulses.

The device under investigation is a ∼1 mm long, single section, DC-biased, and polarization-dependent QDash ML FP laser without saturable absorber. A detailed description of the QDash-based heterostructure, as well as the dimensions of the active core can be found in [4]. The ML laser presents a bias threshold of 18 mA and an average power of 1:6 mW collected by a 0.5 NA lensed fiber when operating at 350 mA and temperature controlled at 25 °C. It features more than 40 longitudinal modes with 0:31 nm intermodal separation, resulting in a 3 dB optical bandwidth of 12 nm centered at 1526 nm. Despite being DC-biased, this passively ML laser generates optical pulses at a 40 GHz repetition rate over a current range between ∼100 and 450 mA [5]. The experimental setup to assess the synchronization performance of the QDash ML laser is shown in Fig. 1. A tunable ML laser (TMLL) at 1550 nm driven by an electrical clock from a pattern generator (PPG) is used to generate a train of 1:6 ps pulses at a 10 GHz repetition rate. As for modulated pulses, a Mach–Zehnder modulator, in combination with the PPG, allows the generation of (231 − 1) long return-to-zero pseudorandom binary sequence at the 10 Gbps base rate. Pulse sequences at 20, 40, 80, and 160 GHz=Gbps are obtained via a fiber-based optical time-domain multiplexer (OMUX) without decorrelation applied between them, so the randomness of the multiplexed channels is not kept. An optical bandpass filter (OBPF-1) set at ∼1550 nm with a 6 nm bandwidth suppresses part of the amplified spontaneous emission of the amplification modules. Pulses at various repetition rates are then injected into the QDash ML laser diode through an optical circulator. Recovered clock pulses from the QDash laser are isolated from injected signals by OBPF-2 set at ∼1530 nm with a 6 nm bandwidth. Output pulses are passively compressed by 450 m single-mode fiber [9]. Temporal traces of the recovered clock pulses (and input pulses) are analyzed with a second harmonic generation frequency-resolved optical gating (FROG) system from Southern Photonics set at 72 fs resolution [10].

An optical sampling oscilloscope (OSO) featuring a re-solution of ∼0:8 ps is used as an aid to ensure the QDash laser operates under external optical synchronization. Indeed, no eye diagrams are retrieved from the OSO in the absence of external locking of the QDash laser because the trigger signal from PPG is not synchronized with the free-running frequency of the laser. Moreover, in comparison to the external synchronization, a shift in the central frequency and a significant increase in the FWHM are ob-served on the 40 GHz beat-tone signal when there is no external locking (resolved by a 50 GHz photodiode and electrical spectrum analyzer).

Eye diagrams and Fourier spectra of the modulated pulses injected into the QDash ML laser are shown in Figs. 2(a)–2(j). In this case, all data are resolved by the optical sampling scope (note that injected signals in Figs. 2(d) and 2(e) appear less discrete due to the 0:8 ps resolution of the OSO). For injected pulses at 20, 40, 80, and 160 Gbps, the spectral components below their cor-responding fundamental frequency (at 20, 40, 80, and 160 GHz, respectively) have been minimized by optimizing the operational conditions of the OMUX in terms of delay and optical power balance between the time-domain multiplexed data streams. Some unwanted components remain for input pulses at 80 and 160 Gbps. However, their amplitude is at least 15 dB below the fundamental component, as shown in Figs. 2(i) and 2(j).

Shape and chirp of both the input pulses and recovered clock are also resolved by the FROG system once the QDash ML laser is externally synchronized. Synchronization is found to be sustained for injected powers between þ6 and þ10 dBm measured by the variable optical attenuator (VOA-1). Fine tuning is achieved by setting a lin-ear state of polarization of the injected beams in close alignment with the eigenaxis of the laser waveguide, while its bias current and temperature are set to ~90 mA and 25 °C, respectively. As shown in Figs. 2(k)–2(o), recovered clock pulses at 40 GHz exhibit a FWHM of ~1:8 ps and nearly linear phase regardless of the repetition rate of the injected pulses. Time domain characteristics of the clock pulses remain unchanged despite the shape and phase variations of input pulses, as evidenced in the insets of Figs. 2(k)–2(o). The complex phase dependence of the input signals is due to the presence of a saturable absorber in the TMLL cavity. In addition, a maximum timing jitter of 0:4 ps is estimated for recovered clock pulses by implementing the method described in [9].

Fourier spectrum of recovered clock pulses exhibits an envelope with a characteristic sinc-like shape, featuring a fundamental component at 40 GHz, as shown in Fig. 3. The power spectral density of components at 10 and 20 GHz is negligible, over 40 dB below the main component, which implies that injected frequencies at 10 and 20 GHz do not create any amplitude modulation in the active locking process achieved by the injection of pulses at 10 and 20 Gbps. In addition, it is worth noting that for optical injection at subharmonic and fundamental data rates, synchronization of the QDash ML laser can be attributed to the 40 GHz component inherently contained in those input signals. However, since such a frequency component has deliberately been minimized for input sequences at 80 and 160 Gbps, the external synchronization can be attributed to the phase-locking mechanism be-tween the fundamental 80 and 160 GHz injected components and the corresponding second (80 GHz) and fourth (160 GHz) harmonics of the QDash laser in free running. This represents a significant feature in the case of injected pulse sequences with repetition rates above the free spectral range of the QDash ML laser since no spectral component at 40 GHz is involved in the synchronization mechanism.

Negligible variations in the time and frequency traces of the recovered 40 GHz pulses are observed for injection of non-modulated pulse streams at the five analyzed repetition rates. Furthermore, performance of the QDash ML laser in terms of the width of injected pulses was not evaluated due to the limitations of the 10 GHz pulse generator used. However, a similar experiment was performed using a cw tunable laser instead of the TMLL, injecting non-return-to-zero pulse sequences into a QDash laser with wavelengths ranging from 1535 to 1550 nm [11].

In summary, synchronization of a 40 GHz QDash ML laser with 10 to 160 GHz non-modulated and 10 to 160 Gbps modulated pulse sequences have been experimentally investigated. Recovered clock pulses have been analyzed in both time and frequency domains. A ~1:8 ps width is measured for recovered clock pulses irrespective of the injected data rate. For injection at 80 and 160 GHz/Gbps, no spectral component at 40 GHz is applied for external synchronization, allowing the implementation of functionalities such as all-optical time demultiplexing and line rate clock recovery (after time-domain multiplexing of recovered clock pulses).

Authors acknowledge Enterprise Ireland under the program CFTD/2009/0303 and the Higher Education Authority Program for Research in Third Level Ins-titutions (2007–2011) via the INSPIRE Programme. S. Philippe acknowledges the Irish Research Council for Science, Engineering and Technology for their support.

References

1. T. Ohno, K. Sato, R. Iga, Y. Kondo, T. Ito, T. Furuta, K. Yoshino, and H. Ito, Electron. Lett. 40, 265 (2004).
2. J. Slovak, C. Bornholdt, J. Kreissl, S. Bauer, M. Biletzke, M. Schlak, and B. Sartorius, IEEE Photon. Technol. Lett. 18, 844 (2006).
3. M. G. Thompson, A. R. Rae, M. Xia, R. V. Penty, and I. H. White, IEEE J. Sel. Top. Quantum Electron. 15, 661 (2009).
4. F. Lelarge, B. Dagens, J. Renaudier, R. Brenot, A. Accard, F. van Dijk, D. Make, O. Le Gouezigou, J.-G. Provost, F. Poingt, J. Landreau, O. Drisse, E. Derouin, B. Rousseau, F. Pommereau, and G.-H. Duan, IEEE J. Sel. Top. Quantum Electron. 13, 111 (2007).
5. S. Latkowski, R. Maldonado-Basilio, and P. Landais, Opt. Express 17, 19166 (2009).
6. J. Renaudier, B. Lavigne, F. Lelarge, M. Jourdran, B. Dagens, O. Legouezigou, P. Gallion, and G.-H. Duan, IEEE Photon. Technol. Lett. 18, 1249 (2006).
7. V. Roncin, A. O'Hare, S. Lobo, E. Jacquette, L. Bramerie, P. Rochard, Q.-T. Le, M. Gay, J.-C. Simon, A. Shen, J. Renaudier, F. Lelarge, and G.-H. Duan, IEEE Photon. Technol. Lett. 19, 1409 (2007).
8. X. Tang, J. C. Cartledge, A. Shen, A. Akrout, and G.-H. Duan, Opt. Lett. 34, 899 (2009).
9. R. Maldonado-Basilio, J. Parra-Cetina, S. Latkowski, and P. Landais, Opt. Lett. 35, 1184 (2010).
10. R. Trebino, K. W. DeLong, D. N. Fittinghoff, J. N. Sweetser, M. A. Krumbugel, B. A. Richman, and D. J. Kane, Rev. Sci. Instrum. 68, 3277 (1997).
11. J. Parra-Cetina, S. Latkowski, R. Maldonado-Basilio, and P. Landais, IEEE Photon. Technol. Lett. PP (2011).

Figures

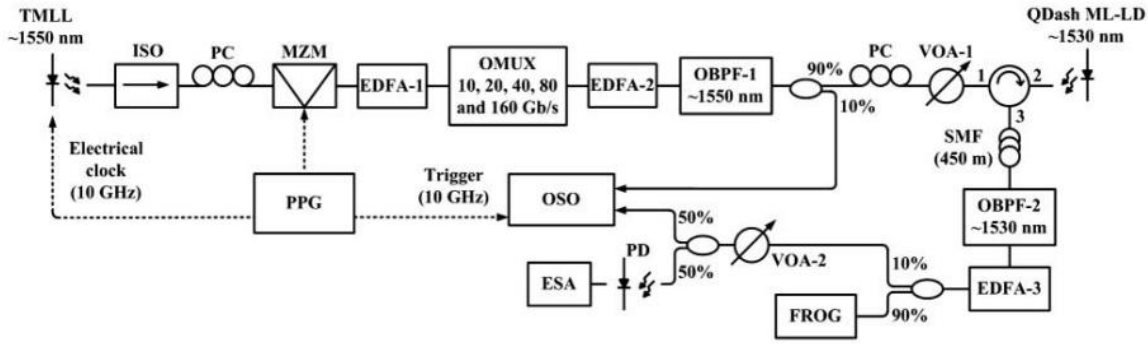

Fig. 1. Experimental setup. ISO, optical isolator; PC, polarization controller; MZM, Mach–Zehnder modulator; EDFA, erbium-doped fiber amplifier; VOA, variable optical attenuator. Full and dotted lines represent optical and electrical links, respectively.

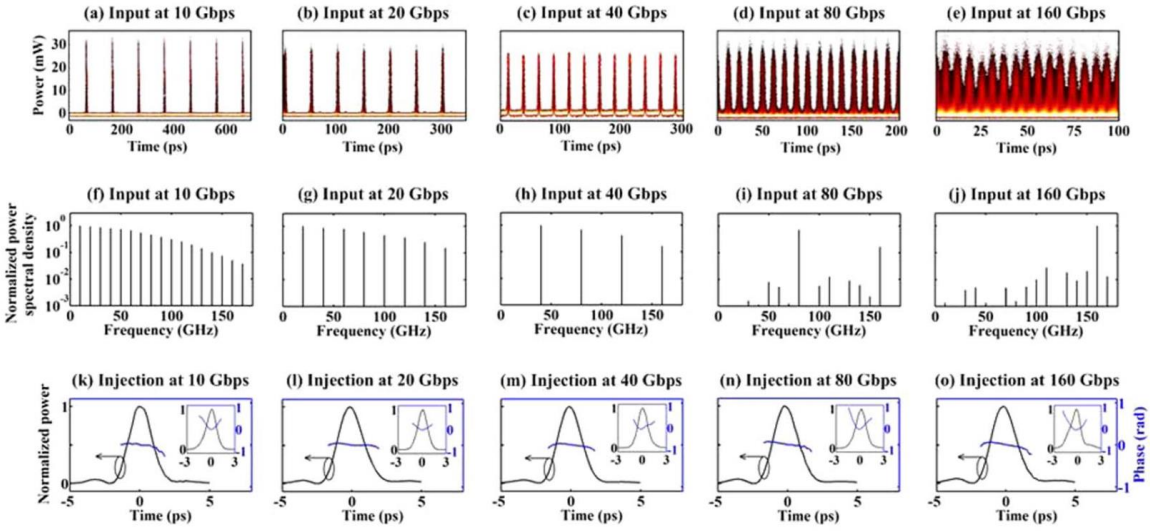

Fig. 2. (Color online) (a)–(e) Eye diagrams and (f)–(j) frequency components of injected pulses at 10, 20, 40, 80, and 160 Gbps resolved by the optical sampling scope. (k)–(o) Time domain (shape and phase) of recovered clock pulses resolved by the FROG system; insets depict detailed shape and phase of injected pulses.

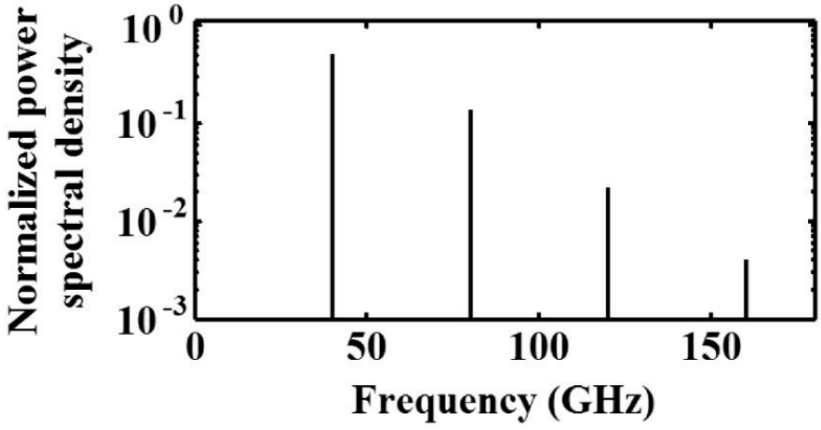

Fig. 3. Frequency components of recovered clock pulses resolved by the optical sampling scope.